

DOI: 10.18721/JPM/12312

УДК 539.126.3

## JET-QUENCHING STUDIES IN ULTRARELATIVISTIC COPPER-GOLD NUCLEI COLLISIONS USING OMEGA MESONS

*A.Ya. Berdnikov, Ya.A. Berdnikov, S.V. Zharko,  
D.O. Kotov, P.V. Radzevich*

Peter the Great St. Petersburg Polytechnic University, St. Petersburg, Russian Federation

In the paper, the measurement data on  $\omega$  meson invariant transverse momentum spectra and nuclear modification factors in collisions of copper and gold nuclei (Cu + Au) at energy of 200 GeV have been presented. The studies were conducted with PHENIX spectrometer at RHIC. The obtained  $\omega$  meson nuclear modification factors were equal (within the uncertainties) to ones derived for  $\pi^0$ ,  $\eta$  and KS mesons and for jets as well in the same collision system. The integrated  $\omega$ -meson nuclear modification factors versus the numbers of nuclei taking part in the nuclei-nuclei interaction, were in agreement (within uncertainties) with the similar dependences for Cu + Au, Au + Au and Cu + Cu collisions at energy of 200 GeV. The analysis of results suggested that the jet-quenching effect was independent (or weakly dependent) of the shape of a nuclear overlap region realized in these systems.

**Keywords:** quark-gluon plasma, jet-quenching effect, nuclear modification factor, omega meson

**Citation:** Berdnikov A.Ya., Berdnikov Ya.A., Zharko S.V., Kotov D.O., Radzevich P.V., Jet-quenching studies in ultrarelativistic copper-gold nuclei collisions using omega mesons, St. Petersburg Polytechnical State University Journal. Physics and Mathematics. 12 (1) (2019) 131–141 DOI: 10.18721/JPM.12312

## ИССЛЕДОВАНИЕ ЭФФЕКТА ГАШЕНИЯ АДРОННЫХ СТРУЙ В СТОЛКНОВЕНИЯХ ЯДЕР МЕДИ И ЗОЛОТА

**С ПОМОЩЬЮ ОМЕГА-МЕЗОНОВ**

*А.Я. Бердников, Я.А. Бердников, С.В. Жарко,  
Д.О. Котов, П.В. Радзевич*

Санкт-Петербургский политехнический университет Петра Великого,  
Санкт-Петербург, Российская Федерация

В статье представлены результаты измерения инвариантных спектров рождения по поперечному импульсу и факторов ядерной модификации  $\omega$ -мезонов в столкновениях ядер меди и золота (Cu + Au) при энергии 200 ГэВ. Исследования проведены с помощью спектрометра PHENIX на коллайдере RHIC. Измеренные значения факторов ядерной модификации  $\omega$ -мезонов равны (в пределах погрешности) значениям, полученным ранее для  $\pi^0$ -,  $\eta$ - и KS-мезонов, а также для адронных струй в той же системе сталкивающихся ядер. Зависимости интегральных факторов ядерной модификации  $\omega$ -мезонов от числа нуклонов, участвующих в ядро-ядерном взаимодействии, совпадают друг с другом (в пределах погрешности) в столкновениях Cu + Au, Au + Au и Cu + Cu при энергии 200 ГэВ. Анализ результатов свидетельствует о независимости (либо слабой зависимости) эффекта гашения адронных струй от формы области ядерного перекрытия, реализуемой в этих системах.

**Ключевые слова:** кварт-глюонная плазма, эффект гашения адронных струй, фактор ядерной модификации, омега-мезон

**Ссылка при цитировании:** Бердников А.Я., Бердников Я.А., Жарко С.В., Котов Д.О., Радзевич П.В. Исследование эффекта гашения адронных струй в столкновениях ядер меди и золота с помощью омега-мезонов // Научно-технические ведомости СПбГПУ. Физико-математические науки. 2019. Т. 3 № .12. С. 143–154. DOI: 10.18721/JPM.12312

## Introduction

Strong interaction of quarks and gluons is characterized by confinement of their color charge, meaning that these particles cannot exist in a free state. However, Shuryak [1] predicted in the 1970s that quark-gluon matter could become deconfined with an increase in its temperature to several hundred MeV. This state was termed quark-gluon plasma (QGP), drawing an analogy with electron-ion plasma. The potential of interaction between quarks and gluons in QGP tends to zero because the average distance between them is small; as a result, their motion is regarded as quasi-free.

Shuryak proposed to use collisions of ultrarelativistic heavy nuclei ( $A + A$ ) for experimental observation of QGP [1], laying the foundations for experiments on collisions of heavy nuclei in accelerators. Attempts to detect QGP were made in the 1980s and 1990s at Bevalac (Lawrence Berkeley National Laboratory, USA), AGS (Brookhaven National Laboratory, USA) and SPS (CERN, Switzerland) accelerators. However, the first systematic observations hinting at the existence of QGP were made at the Relativistic Heavy Ions Collider (Brookhaven National Laboratory, USA) [4–5]. QGP production was later confirmed at the Large Hadron Collider (CERN, Switzerland) [6–8].

Strong suppression of hadron yield in the region of high transverse momenta ( $p_T > 4–6$  GeV/c), compared with the yields measured in proton-proton ( $p + p$ ) interactions, is a signature for QGP production in ( $A + A$ ) collisions [5]. No such suppression was observed for direct photons in ( $A + A$ ) collisions and for hadrons in deuteron-nucleus ( $d + A$ ) interactions [5]. Suppression of hadron yields is called jet quenching; it is associated with energy loss

of hard partons passing through quark-gluon plasma [9].

Typical kinetic energies of beams of ultrarelativistic nuclei at RHIC have by values of the order of 100 GeV/nucleon, corresponding to de Broglie wavelength (about  $10^{-4}$  fm). Thus, only a part of the nucleons in the colliding nuclei participate in a single event of a nucleus-nucleus interaction and subsequent production of QGP (participant nucleons), while the remaining nucleons escape the colliding nuclei and leave the interaction region (spectator nucleons). The overlap of colliding nuclei is used to classify the collisions (events) by centrality, measured as a percentage: collisions with a large overlap, a large number of participants  $N_{part}$  and a small impact parameter  $b$  correspond to centralities of the order of 0–20%, collisions with small overlap and small  $N_{part}$  are of the order of 60–90%. The central and peripheral nucleus-nucleus collisions are schematically shown in Fig. 1.

Quantitative description of the jet quenching effect is commonly obtained using the nuclear modification factor, given by the formula

$$R_{AA}(p_T) = \frac{1}{N_{coll}} \frac{dN_{AA}/dp_T}{dN_{pp}/dp_T}, \quad (1)$$

where  $dN_{AA}/dp_T$ ,  $dN_{pp}/dp_T$  are the hadron yields in ( $A + A$ ) and ( $p + p$ ) collisions, respectively, in a given range of transverse momenta  $p_T$ ;  $N_{coll}$  is the number of binary inelastic nucleon-nucleon interactions.

If  $R_{AA} = 1$ , then the nucleus-nucleus collision can be interpreted as simple superposition of nucleon-nucleon interactions. The opposite case suggest the presence of collective medium effects; in fact, the effects occurring both in

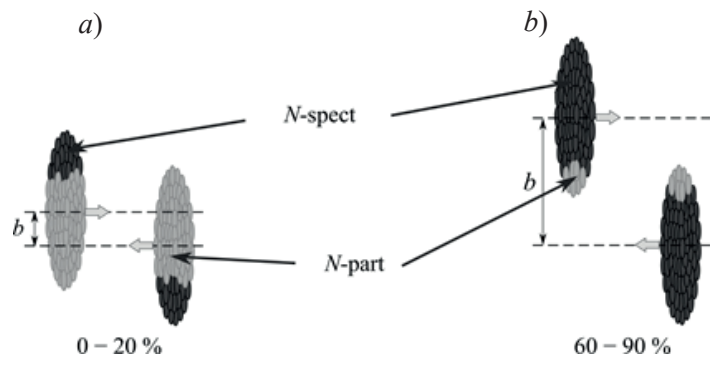


Fig. 1. Geometric pattern of nucleus-nucleus collisions: central (a) and peripheral (b); centralities (%) are given;  $N_{part}$ ,  $N_{spect}$  are participant and spectator nucleons, respectively;  $b$  is the impact parameter



$p(d) + A$  and  $A + A$  interactions are effects of cold nuclear matter, while jet quenching is the effect of hot nuclear matter and occurs only in  $(A + A)$  systems.

Measuring the nuclear modification factors of different types of hadrons in different systems of colliding nuclei is one of the main tools for analysis of collective effects, including jet quenching depending on the properties of these hadrons (mass, spin, quark composition, etc.). For example,  $\omega$  mesons, like  $\pi^0$  mesons, consist of quarks and antiquarks of the first generation ( $u, d$ ), but at the same time,  $\omega$  mesons belong to vector meson resonances and have a unit spin, while  $\pi^0$  mesons are pseudoscalar particles with zero spin. Previous studies of  $\omega$  meson production were carried out in symmetric binary collisions of gold nuclei ( $Au + Au$ ) [10] and copper nuclei ( $Cu + Cu$ ) [10].

The system of colliding copper and gold nuclei ( $Cu + Au$ ) at  $\sqrt{s_{NN}} = 200$  GeV is of particular interest for systematic study of the properties of QGP. It is the only asymmetric collision system of ultrarelativistic heavy nuclei characterized by a special overlap geometry that is different from the  $Cu + Cu$  and  $Au + Au$  systems. Exploring the production of  $\omega$  mesons in the  $Cu + Au$  collision system should make it possible to impose additional restrictions on the parameters of a number of phenomenological models describing hadron energy losses in QGP [11–19].

The paper reports on measurements of invariant production spectra depending on transverse momentum and nuclear modification factors of  $\omega$  mesons in collisions of copper and gold nuclei ( $Cu + Au$ ) at  $\sqrt{s_{NN}} = 200$  GeV.

### Experimental setup

Production of  $\omega$  mesons was measured using a PHENIX spectrometer [20] at RHIC. A system of beam-beam counters (BBC) [21] was used to determine the centrality, the coordinate of the event along the beam axis ( $z_{vertex}$ ) [21], collision time [21], and also to fire the MB trigger [21, 22] recording signals from the detector subsystems of the PHENIX spectrometer if at least one inelastic nucleon-nucleon interaction is detected. Two groups of BBC counters covered a range of  $3.1 < |\eta| < 3.9$  in pseudo-rapidity and a full azimuthal angle. The counters are located along the beam axis 144 cm away from the nominal point of intersection. Each group consists of 64 counters, which are Cherenkov detectors with a quartz radiator 3.00 cm thick and 2.54 cm in radius, and mea-

sures the electric charge deposited by spectator nucleons. The centrality  $C$  of this event is found by the expression

$$C = \varepsilon_{MB} (1 - \delta(Q_{BBC})), \quad (2)$$

where  $\varepsilon_{MB} = 93 \pm 3\%$  is the efficiency of the MB trigger;  $Q_{BBC}$  is the charge detected in this event;  $\delta(Q_{BBC})$  is the fraction of events for which the electric charge detected is less than  $Q_{BBC}$ .

The yield of  $\omega$  mesons was measured in four centrality classes of ( $Cu + Au$ ) collisions: 0–20, 20–40, 40–60, 60–90%, and in a class without centrality specified: 0–93%. Geometrical parameters of nucleus-nucleus collisions, such as  $N_{part}$  and  $N_{coll}$  are determined by Monte Carlo simulation of the BBC responses based on the Glauber model [23].

A system of electromagnetic calorimeters (EMCal) [24] was used to determine the energy and the point of incidence of gamma rays generated in the decays of neutral mesons ( $\pi^0, \eta, K_S, \omega$ ). It consists of two subsystems based on different technologies: PbSc, a subsystem of scintillator sampling calorimeters with a lead absorber and PbGl, a subsystem of lead-glass Cherenkov calorimeters; these subsystems are distributed in six and two sectors of the calorimeter, respectively. Each sector of the electromagnetic calorimeter covers a  $|\eta| < 0.35$  region in pseudo-rapidity and  $\Delta\phi = 22.5^\circ$  in azimuthal angle; the PbSc subsystem is located 5.1 m, and PbGl 5.4 m away from the beam axis of colliding heavy nuclei. The segmentation of the  $\delta\phi \times \delta\eta$  sectors of the PbSc and PbGl subsystems was approximately  $0.010 \times 0.010$  and  $0.008 \times 0.008$ , respectively. Construction and performance of the electromagnetic calorimeter system is discussed in detail in [24].

### Reconstruction of $\omega$ meson yields

The  $\omega$  mesons are reconstructed via the  $\omega \rightarrow \pi^0 + \gamma$  channel by analyzing the distributions of  $\pi^0\gamma$  pairs over invariant mass  $m_{inv}$ . The invariant mass for each  $\pi^0\gamma$  pair is found by the expression

$$m_{inv} = \sqrt{E^2 - \mathbf{p}^2}, \quad (3)$$

where  $E$  and  $\mathbf{p}$  are the total energies and momenta of the candidates detected for the role of daughter  $\pi^0$  mesons ( $\pi^0$  candidates) and daughter  $\gamma$  quanta ( $\gamma$  candidates).

A number of kinematic constraints are imposed on the characteristics of the  $\pi^0\gamma$  pairs and the  $\pi^0$  candidates producing them to improve the signal-to-background ratio for  $\omega$  mesons.

Clusters detected in an electromagnetic calorimeter are associated with  $\gamma$ -quanta if the energy released in them exceeds 0.4 GeV and their shape satisfies standard restrictions [24]. These restrictions make it possible to discriminate a significant fraction of the clusters deposited by charged hadrons. The  $\pi^0$  candidates are produced via the  $\pi^0 \rightarrow \gamma + \gamma$  channel. Both  $\gamma$  quanta in the  $\gamma\gamma$  pair should be detected in the same sector of the electromagnetic calorimeter, and their energies,  $E_{\gamma 1}$  and  $E_{\gamma 2}$ , should satisfy the ratio

$$\frac{|E_{\gamma 1} - E_{\gamma 2}|}{E_{\gamma 1} + E_{\gamma 2}} \leq 0.8. \quad (4)$$

The transverse momentum of the  $\pi^0$  candidate detected in the PbSc or PbGl subsystem should be in the range of 2–11 (14)  $\text{GeV}/c$ . The lower bound is imposed to further increase the signal-to-background ratio for  $\omega$  mesons. The upper bound should exclude merging of electromagnetic clusters (occurring because it is impossible to separately detect two daughter  $\gamma$  quanta as the angle between their momenta is small). This effect is observed in the PbGl-sub-

system for high transverse momenta due to finer segmentation, and, as a consequence, better discrimination between the clusters.

Next,  $\pi^0$  candidates are selected in a given range by the inequality

$$|m_{\gamma\gamma} - M_{\pi^0}(p_T)| \leq 2\sigma_{\pi^0}(p_T), \quad (5)$$

where  $m_{\gamma\gamma}$  is the invariant mass of the  $\gamma\gamma$  pair forming the  $\pi^0$  candidate;  $M_{\pi^0}$ ,  $\sigma_{\pi^0}$  are the parameterizations of the position and width of the peaks (respectively) from  $\pi^0$  mesons in distributions over  $m_{\gamma\gamma}$  (the measured mass).

The energies of  $\gamma$  quanta in pairs producing  $\pi^0$  candidates and satisfying constraint (5) are adjusted to reduce the measured masses to tabulated values [25] for increasing the signal-to-background ratio for  $\omega$  mesons by eliminating the spread in the measured masses of  $\pi^0$  candidates.

The energy of the  $\gamma$ -candidate for a reconstructed  $\pi^0\gamma$  pair should be no lower than 1 GeV;  $\pi^0$  and  $\gamma$  candidates should be detected in the same arm (west or east) of the PHENIX spectrometer and satisfy the condition

$$|\cos \theta^*| \leq 0.6 \quad (6)$$

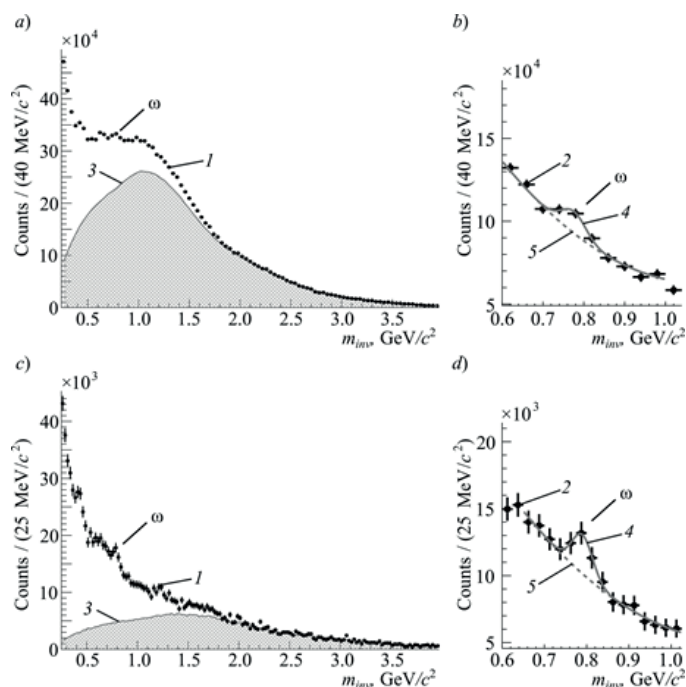


Fig. 2. Examples of initial (a, c) and processed (b, d) experimental distributions of  $\pi^0\gamma$  pairs by invariant mass in ranges of 6–7  $\text{GeV}/c$  (a, b) and 8–10  $\text{GeV}/c$  (c, d):

1, 2 correspond to initial and final experimental points, respectively; 3 to functions of uncorrelated background component; 4, 5 to functions approximating signal + background and background, respectively



where  $\theta^*$  is the angle between the direction of the  $\pi^0$  meson in rest frame of the  $\pi^0\gamma$  pair and the direction of this pair in laboratory frame. Restriction (6) is essentially similar to restriction (4), adopted for  $\gamma\gamma$  pairs.

Invariant mass distributions are formed in different transverse momentum ranges and centrality classes. The background in invariant mass distributions of  $\pi^0\gamma$  pairs consists of correlated and uncorrelated components. The first is generated by decay products of other particles (for example,  $\eta$ ,  $\eta'$ , and  $K_S$  mesons). The second is associated with random combinations of candidate particles and is estimated

using event mixing: an additional (uncorrelated) distribution is formed for each distribution obtained over the invariant mass, so that ten  $\gamma$  candidates from other events with close values of centrality and  $z_{\text{vertex}}$  coordinate are assigned to each  $\pi^0$  candidate. Using ten  $\gamma$  candidates instead of one can significantly increase the statistical significance of the uncorrelated distribution. The function of the uncorrelated background component obtained this way is normalized to the invariant mass distribution in the region  $m_{\text{inv}} > 2 \text{ GeV}/c^2$  and is subtracted from it. Examples of final invariant mass distributions of  $\pi^0\gamma$  pairs are shown in Fig. 2.

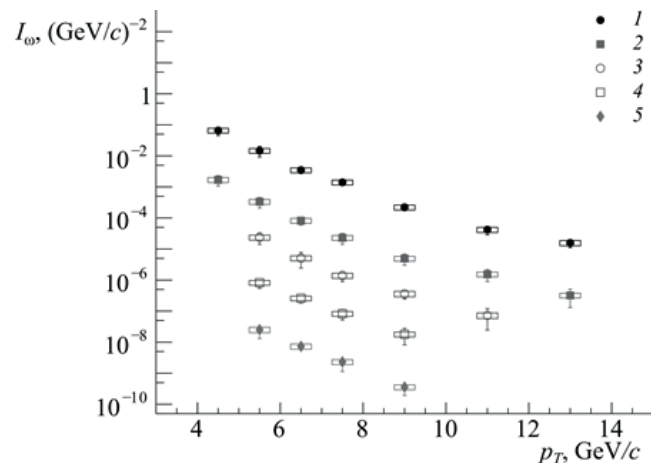


Fig. 3. Invariant spectra of  $\omega$  meson production with respect to transverse momentum in (Cu + Au) collisions in different centrality classes, %:  
 0–20 (2), 20–40 (3), 40–60 (4), 60–90 (5), and without centrality specified (1).  
 The points are scaled by  $10^1$  (2),  $10^0$  (3),  $10^{-1}$  (4),  $10^{-2}$  (5) and  $10^3$  (1)

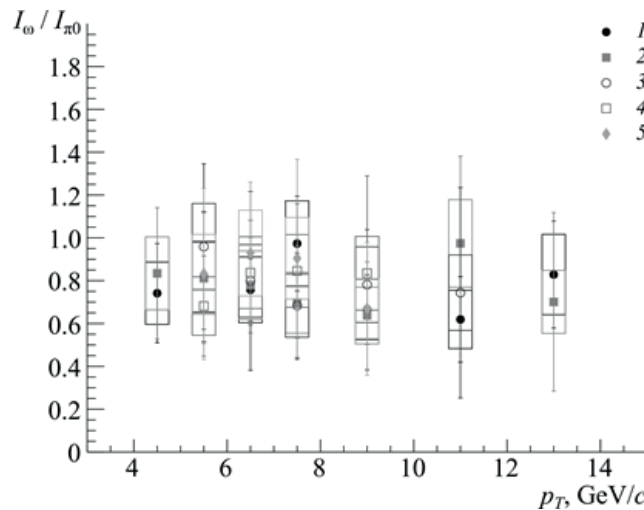


Fig. 4.  $I_{\omega}/I_{\pi^0}$  ratios as functions of transverse momentum in (Cu + Au) collisions in different centrality classes, %: 0–20 (2), 20–40 (3), 40–60 (4), 60–90 (5), and without centrality specified (1)

The functions of the uncorrelated background component were estimated here by the event mixing method. The peaks correspond to signals from  $\omega$  mesons.

To measure the yield of  $\omega$  mesons, the distributions are fitted to a sum of a Gaussian (approximating the signal) and a second-order polynomial (approximating the residual correlated background component in the region around the signal). The number of  $\omega$  mesons detected is found by the area (integral) under the Gaussian.

The invariant yield, i.e., the number of mesons generated at the vertex of nucleus-nucleus collisions, is found by correcting the number of  $\omega$ -mesons detected for limited acceptance, the detector effects of the calorimeter and for the kinematic constraints used with the reconstruction efficiency. Reconstruction efficiency is estimated through Monte Carlo simulation of the experimental setup in GEANT3.

The invariant yield of  $\omega$  mesons is determined by the formula

$$I_{\omega} = \frac{1}{N_{ev}} \frac{d^2 N}{2\pi p_T dp_T dy} = \frac{N_{\omega}}{2\pi p_T \Delta p_T N_{ev} \varepsilon_{rec} \text{BR}}, \quad (7)$$

where  $N_{\omega}$  is the number of  $\omega$  mesons reconstructed;  $\varepsilon_{rec}$  is the reconstruction efficiency;  $N_{ev}$  is the number of events analyzed,  $\text{BR}$  is the branching ratio for the  $\omega \rightarrow \pi^0 + \gamma$  channel,  $\text{BR} = 8.40 \pm 0.22\%$  [25].

The systematic uncertainty in measuring the invariant yield of  $\omega$  mesons was estimated by comparing the standard yields with the values obtained by varying the fitting parameters of invariant mass distributions, the simulation parameters (for example, the absolute energy scale and energy resolution of the calorimeter) and the kinematic constraints used. The main sources of systematic uncertainty are possible errors in choosing the fitting parameters (for example, subtracting the uncorrelated background component or choosing the order of the polynomial describing the residual background) of invariant mass distributions for  $\pi^0\gamma$  pairs (7–15% for different transverse momenta and centralities), a possible discrepancy between the algorithms for describing cluster shape (9.2%) and photon conversion in detector materials (7.8%) in the Monte Carlo model and real data.

The main sources of systematic uncertainty are:

- 1) possible errors in choosing the fitting pa-

rameters for invariant mass distributions of the  $\pi^0\gamma$  pairs (for example, excluding the uncorrelated background component, choosing the order of the polynomial describing the residual background);

2) possible discrepancy between the algorithms for describing cluster shape in detector materials;

3) possible discrepancy between the operation of algorithms for describing photon conversion in detector materials in the Monte Carlo model and real data.

Quantitatively speaking, the systematic uncertainties resulting from the above factors amount to 7–15% (for different transverse momenta and centralities), 9.2% and 7.8%, respectively.

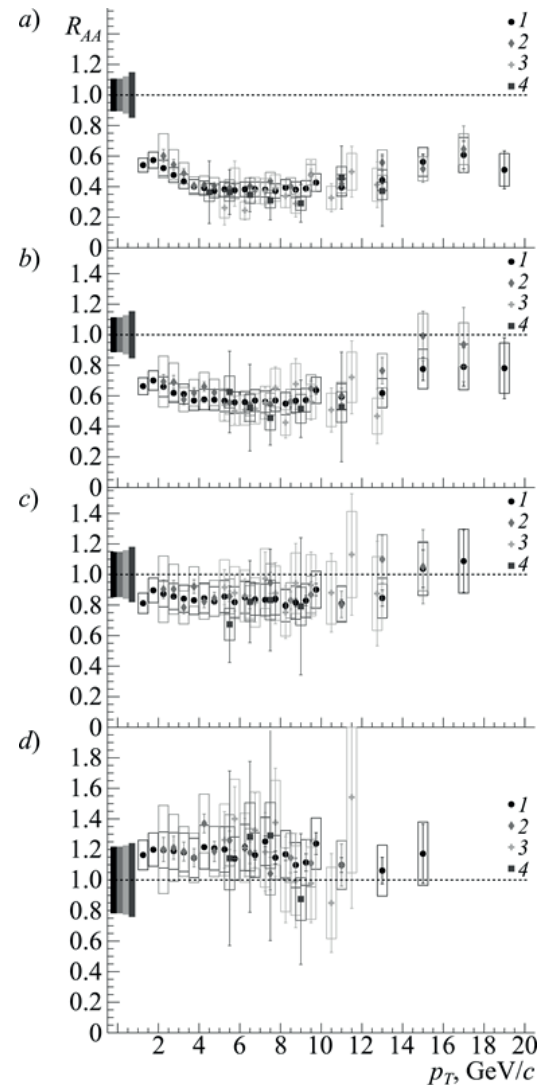


Fig. 5. Nuclear modification factors of  $\pi^0$  (1) [27, 28],  $\eta$  (2) [27, 28],  $K_s$  (3) and  $\omega$  (4) mesons as functions of transverse momentum in  $(\text{Cu} + \text{Au})$  collisions at  $\sqrt{s_{NN}} = 200$  GeV in different centrality classes, %: 0–20 (a), 20–40 (b), 40–60 (c), 60–90 (d)



## Results and discussion

Invariant spectra for production of  $\omega$  mesons, measured as a function of their transverse momentum in different centrality classes of Cu + Au collisions at  $\sqrt{s_{NN}} = 200$  GeV are shown in Fig. 3. The transverse momentum ranges of the measured spectra are limited because it is impossible to separate the signal from the background (lower bound) and because there are insufficient data for measuring the yields (upper bound). The bars and rectangles near the dots in Figs. 3–6 correspond to absolute values of statistical and systematic uncertainties.

Fig. 4 shows the ratios of  $\omega$  meson to  $\pi^0$  meson yields,  $I_\omega/I_{\pi^0}$ , measured in different ranges of transverse momenta and different centrality classes of Cu + Au collisions at  $\sqrt{s_{NN}} = 200$  GeV. The yields of  $\pi^0$  mesons previously measured in Cu + Au collisions are used as the denominator [27, 28]. The relative statistical and systematic uncertainties for the  $I_\omega/I_{\pi^0}$  ratios are found as quadratic sums of relative uncertainties in measuring  $\omega$  and  $\pi^0$  meson yields. Analysis of the obtained data indicates that the measured ratios do not depend on transverse momentum and centrality within the measurement uncertainty. The  $I_\omega/I_{\pi^0}$  ratios lie in the range of about 0.7–0.8, which coincides (within the uncertainty) with the ratios previously measured in the PHENIX experiment in  $p + p$ ,  $d + Au$ , Cu + Cu and Au + Au collisions at  $\sqrt{s_{NN}} = 200$  GeV [10].

Fig. 5 shows the nuclear modification factors of  $\pi^0$  [27, 28],  $\eta$  [27, 28],  $K_s$  and  $\omega$  mesons measured in different centrality classes of (Cu + Au) collisions at  $\sqrt{s_{NN}} = 200$  GeV. Rectangles near the points correspond to absolute values of

the systematic measurement uncertainty with unknown correlation with respect to transverse momentum. Rectangles near unity correspond to the relative systematic uncertainty, fully correlated to the transverse momentum. The nuclear modification factor of  $\omega$  mesons is calculated by substituting the product of the fitted production spectrum of  $\pi^0$  mesons measured in the system of ( $p + p$ ) interactions at  $\sqrt{s_{NN}} = 200$  GeV used as the denominator in formula (1) with the ratio  $I_\omega/I_{\pi^0} = 0.81 \pm 0.02 \pm 0.07$  obtained in the same system [10].

The measured nuclear modification factors of  $\pi^0$ ,  $\eta$ ,  $K_s$  and  $\omega$  mesons in the system of (Cu + Au) collisions coincide within the uncertainty in transverse momentum ranges and centrality classes. The given factors for these mesons in the region  $p_T > 10$  GeV/c in different centrality classes also coincide with those for the jets measured previously in (Cu + Au) collisions [29].

The nuclear modification factor does not depend on the type of mesons ( $\pi^0$ ,  $\eta$ ,  $K_s$ ,  $\omega$ ), suggesting that jet quenching in (Cu + Au) collisions occurs at the parton level, i.e., hard partons in quark-gluon plasma lose energy before they are fragmented into jets.

Fig. 6 shows the dependences of the integral nuclear modification factor of  $\omega$  mesons as function of  $N_{part}$  in the Cu + Au, Au + Au [10] and Cu + Cu systems [10] at  $\sqrt{s_{NN}} = 200$  GeV.

The above dependences coincide within the measurement uncertainty for different systems of colliding nuclei, which indicates that jet quenching in the Cu + Au, Au + Au and Cu + Cu systems at  $\sqrt{s_{NN}} = 200$  GeV is independent of the shape of overlap in these systems.

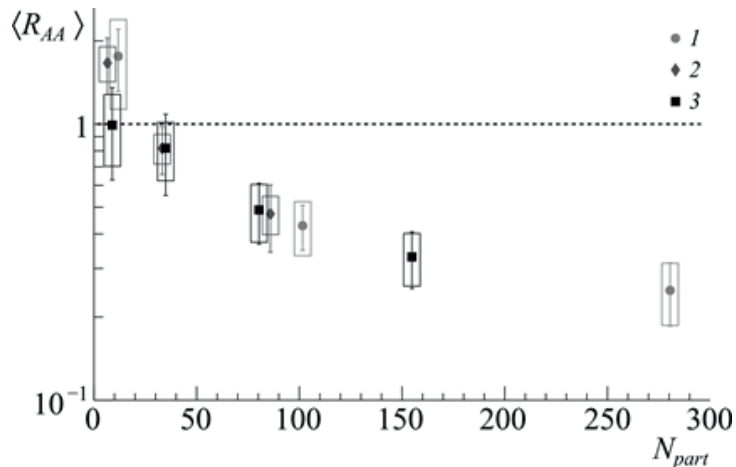


Fig. 6. Integral nuclear modification factor of  $\omega$  mesons as function of  $N_{part}$  in (Au + Au) (1) [10], (Cu + Cu) (2) [10] and (Cu + Au) collisions (3) at  $\sqrt{s_{NN}} = 200$  GeV

## Conclusion

The PHENIX collaboration measured invariant production spectra of  $\omega$  mesons as functions of transverse momentum and nuclear modification factor, as well as ratios of  $\omega$  meson to  $\pi^0$  meson yields in (Cu + Au) collisions at  $\sqrt{s_{NN}} = 200$  GeV depending on transverse momentum and centrality.

The  $I_\omega/I_{\pi^0}$  ratios do not depend on centrality and transverse momentum within the measurement uncertainty. These ratios have the same order of magnitude ( $\sim 0.7$ – $0.8$ ) in collisions of copper and gold nuclei at  $\sqrt{s_{NN}} = 200$  GeV as are the ratios measured previously in  $p + p$ ,  $d + Au$ ,  $Au + Au$  and  $Cu + Cu$  systems at  $\sqrt{s_{NN}} = 200$  GeV.

The nuclear modification factors measured for  $\pi^0$ ,  $\eta$ ,  $K_s$  and  $\omega$  mesons in collisions of copper and gold nuclei coincide within the uncertainty in different centrality classes and trans-

verse momentum ranges, and are also equal to the nuclear modification factors of hadron jets measured in the same collision system in the corresponding centrality classes. This suggests that energy losses of hard partons in (Cu + Au) collisions occur in QGP before they are fragmented into hadron jets. Integral nuclear modification factors of  $\omega$  mesons measured in Cu + Au, Au + Au and Cu + Cu collisions at  $\sqrt{s_{NN}} = 200$  GeV coincide within the measurement uncertainty at close values of  $N_{part}$ , suggesting that jet quenching in the Cu + Au, Au + Au and Cu + Cu systems at  $\sqrt{s_{NN}} = 200$  GeV is independent (or only weakly dependent) of the shape of the overlap.

The results of this study were obtained within the framework of State Task of the Ministry of Education and Science of Russian Federation 3.1498.2017/4.6.

## REFERENCES

1. Shuryak E.V., Quantum chromodynamics and the theory of super dense matter, Physics Reports. 61 (1980) (2) 71–158.
2. Arsene I., Dearden I.G., Beavis D., et al., Quark gluon plasma and color glass condensate at RHIC? The perspective from the BRAHMS experiment, Nuclear Physics, A. 757 (2005) (1–2) 1–27.
3. Back B.B., Baker M.D., Ballintijn M., et al., The PHOBOS perspective on discoveries at RHIC Nuclear Physics, A. 757 (2005) (1–2) 28–101.
4. Adams J., Aggarwal M.M., Ahammed Z., et al., Experimental and theoretical challenges in the search for the quark gluon plasma: the STAR Collaboration's critical assessment of the evidence from RHIC collisions, Nuclear Physics, A. 757 (2005) (1–2) 102–183.
5. Adcox K., Adler S.S., Afanasiev S., et al., Formation of dense partonic matter in relativistic nucleus-nucleus collisions at RHIC: experimental evaluation by the PHENIX Collaboration, Nuclear Physics, A. 757 (2005) (1–2) 184–283.
6. Chatrchyan S., Khachatryan V., Sirunyan A.M., et al., Study of high- $p_T$  charged particle suppression in Pb–Pb compared to  $p + p$  collisions at  $\sqrt{s_{NN}} = 2.76$  TeV, The European Physical Journal, C. 72 (2012) (3) 1945.
7. Aad G., Abbott B., Abdallah J., et al., Measurement of the jet radius and transverse momentum dependence of inclusive jet suppression in lead-lead collisions at  $\sqrt{s_{NN}} = 2.76$  TeV with the ATLAS detector, Physics Letters, B. 719 (2013) (4–5) 220–241.
8. Abelev B., Adam J., Adamova D., et al., Centrality dependence of charged particle production at large transverse momentum in Pb–Pb collisions at  $\sqrt{s_{NN}} = 2.76$  TeV, Physics Letters, B. 720 (2013) (1–3) 52–62.
9. Bjorken J.D., Energy loss of energetic partons in quark-gluon plasma: possible extinction of high  $p(t)$  jets in hadron-hadron collisions, (1982) FERMILAB-PUB-82-059-T.
10. Adare A., Afanasiev S., Aidala C., et al., Production of  $\omega$  mesons in  $p + p$ ,  $d + Au$ ,  $Cu + Cu$ , and  $Au + Au$  collisions at  $\sqrt{s_{NN}} = 200$  GeV, Physical Review, C. 84 (2011) (4) 044902.
11. Cao S., Luo T., Qin G.Y., et al., Linearized Boltzmann transport model for jet propagation in the quark-gluon plasma: heavy quark evolution, Physical Review, C. 94 (2016) (1) 014909.
12. Cao S., Park C., Barbieri R.A., et al., Multistage Monte Carlo simulation of jet modification in a static medium, Physical Review, C. 96 (2017) (2) 024909.
13. Elayavalli R.K., Zapp K.C., Medium response in JEWEL and its impact on jet shape observables in heavy ion collisions, Journal of High Energy Physics. 2017 (2017) (7) 141.
14. Park C., Jeon S., Gale C., Jet modification with medium recoil in quark-gluon plasma, Nuclear Physics, A. 982 (2019) (February) 643–646.
15. He Y., Luo T., Wang X.N., et al., Linear Boltzmann transport for jet propagation in the quark-gluon plasma: elastic processes and medium



recoil, *Physical Review, C*. 91 (2015) (5) 054908.

16. **Chien Y.T., Vitev I.**, Towards the understanding of jet shapes and cross sections in heavy ion collisions using soft-collinear effective theory, *Journal of High Energy Physics*. 2016 (2016) (5) 23.
17. **Chien Y.T., Emerman A., Kang Z.B., et al.**, Jet quenching from QCD evolution, *Physical Review, D*. 2016 (93) (7) 074030.
18. **Ghiglieri J.**, Energy loss at NLO in a high-temperature Quark-Gluon Plasma, *Nuclear Physics, A*. 956 (2017) (December) 801–804.
19. **Djordjevic M., Zicic D., Blagojevic B., et al.**, Dynamical energy loss formalism: from describing suppression patterns to implications for future experiments, *Nuclear Physics, A*. 982 (2019) (February) 699–702.
20. **Adcox K., Adler S.S., Aizama M., et al.**, PHENIX detector overview, *Nuclear Instruments and Methods in Physics Research, Section A: Accelerators, Spectrometers, Detectors and Associated Equipment*. 499 (2003) (2–3) 469–479.
21. **Allen M., Bennett M.J., Bobrek M., et al.**, PHENIX inner detectors, *Nuclear Instruments and Methods in Physics Research, Section A: Accelerators, Spectrometers, Detectors and Associated Equipment*. 499 (2003) (2–3) 549–559.
22. **Adler S.S., Allen M., Alley G., et al.**, PHENIX on-line systems, *Nuclear Instruments and Methods in Physics Research, Section A: Accelerators, Spectrometers, Detectors and*
- Associated Equipment. 499 (2003) (2–3) 560–592.
23. **Miller M.L., Reygers K., Sanders S.J., et al.**, Glauber modeling in high-energy nuclear collisions, *Annual Review of Nuclear and Particle Science*. 57 (2007) 205–243.
24. **Aphecetche L., Awes T.C., Banning J., et al.**, PHENIX calorimeter, *Nuclear Instruments and Methods in Physics Research, Section A: Accelerators, Spectrometers, Detectors and Associated Equipment*. 499 (2003) (2–3) 521–536.
25. **Tanabashi M., Hagiwara K., Hikasa K., et al.**, Review of particle physics, *Physical Review, D*. 98 (2018) (3) 030001.
26. **Brun R., Hagelberg R., Hansroul M., et al.**, Geant: simulation program for particle physics experiments. User guide and reference manual, Preprint CERN, (1978) CERN-DD-78-2-REV.
27. **Zharko S. (PHENIX Collaboration)**, Studying parton energy loss using meson production in Large Collision Systems with PHENIX, *Nuclear Physics, A*. 967 (2017) (November) 552–555.
28. **Aidala C., Ajitanand N.N., Akiba Y., et al.**, Production of  $\pi^0$  and  $\eta$  mesons in Cu + Au collisions at  $\sqrt{s_{NN}} = 200$  GeV, *Physical Review, C*. 98 (2018) (5) 054903.
29. **Timilsina A. (PHENIX Collaboration)**, PHENIX results on reconstructed jets in p + p and Cu + Au collisions, *Nuclear Physics, A*. 956 (2016) (December) 637–640.

Received 13.03.2019, accepted 01.04.2019.

## THE AUTHORS

### BERDNIKOV Alexander Ya.

*Peter the Great St. Petersburg Polytechnic University*  
29 Politehnicheskaya St., St. Petersburg, 195251, Russian Federation  
alexber@phmf.spbstu.ru

### BERDNIKOV Yaroslav A.

*Peter the Great St. Petersburg Polytechnic University*  
29 Politehnicheskaya St., St. Petersburg, 195251, Russian Federation  
berdnikov@spbstu.ru

### ZHARKO Sergei V.

*Peter the Great St. Petersburg Polytechnic University*  
29 Politehnicheskaya St., St. Petersburg, 195251, Russian Federation  
zharkosergey94@gmail.com

KOTOV Dmitry O.

*Peter the Great St. Petersburg Polytechnic University*

29 Politehnicheskaya St., St. Petersburg, 195251, Russian Federation

dmitriy.kotov@gmail.com

RADZEVICH Pavel V.

*Peter the Great St. Petersburg Polytechnic University*

29 Politehnicheskaya St., St. Petersburg, 195251, Russian Federation

radzevichp@gmail.com

**СПИСОК ЛИТЕРАТУРЫ**

1. **Shuryak E.V.** Quantum chromodynamics and the theory of super dense matter // Physics Reports. 1980. Vol. 61. No. 2. Pp. 71–158.
2. **Arsene I., Dearden I.G., Beavis D., et al.** Quark gluon plasma and color glass condensate at RHIC? The perspective from the BRAHMS experiment // Nuclear Physics. A. 2005. Vol. 757. No. 1–2. Pp. 1–27.
3. **Back B.B., Baker M.D., Ballintijn M., et al.** The PHOBOS perspective on discoveries at RHIC // Nuclear Physics. A. 2005. Vol. 757. No. 1–2. Pp. 28–101.
4. **Adams J., Aggarwal M.M., Ahammed Z., et al.** Experimental and theoretical challenges in the search for the quark gluon plasma: the STAR Collaboration's critical assessment of the evidence from RHIC collisions // Nuclear Physics. A. 2005. Vol. 757. No. 1–2. Pp. 102–183.
5. **Adcox K., Adler S.S., Afanasiev S., et al.** Formation of dense partonic matter in relativistic nucleus-nucleus collisions at RHIC: experimental evaluation by the PHENIX Collaboration // Nuclear Physics. A. 2005. Vol. 757. No. 1–2. Pp. 184–283.
6. **Chatrchyan S., Khachatryan V., Sirunyan A.M., et al.** Study of high- $p_T$  charged particle suppression in Pb – Pb compared to  $p + p$  collisions at  $\sqrt{s_{NN}} = 2.76$  TeV // The European Physical Journal. C. 2012. Vol. 72. No. 3. P. 1945.
7. **Aad G., Abbott B., Abdallah J., et al.** Measurement of the jet radius and transverse momentum dependence of inclusive jet suppression in lead-lead collisions at  $\sqrt{s_{NN}} = 2.76$  TeV with the ATLAS detector // Physics Letters. B. 2013. Vol. 719. No. 4–5. Pp. 220–241.
8. **Abelev B., Adam J., Adamova D., et al.** Centrality dependence of charged particle production at large transverse momentum in Pb–Pb collisions at  $\sqrt{s_{NN}} = 2.76$  TeV // Physics Letters. B. 2013. Vol. 720. No. 1–3. Pp. 52–62.
9. **Bjorken J.D.** Energy loss of energetic partons in quark-gluon plasma: possible extinction of high  $p(t)$  jets in hadron-hadron collisions. 1982. FermiLab-Pub-82-059-T.
10. **Adare A., Afanasiev S., Aidala C., et al.** Production of  $\omega$  mesons in  $p + p$ ,  $d + \text{Au}$ ,  $\text{Cu} + \text{Cu}$ , and  $\text{Au} + \text{Au}$  collisions at  $\sqrt{s_{NN}} = 200$  GeV // Physical Review. C. 2011. Vol. 84. No. 4. P. 044902.
11. **Cao S., Luo T., Qin G.Y., et al.** Linearized Boltzmann transport model for jet propagation in the quark-gluon plasma: heavy quark evolution // Physical Review. C. 2016. Vol. 94. No. 1. P. 014909.
12. **Cao S., Park C., Barbieri R.A., et al.** Multistage Monte Carlo simulation of jet modification in a static medium // Physical Review. C. 2017. Vol. 96. No. 2. P. 024909.
13. **Elayavalli R.K., Zapp K.C.** Medium response in JEWEL and its impact on jet shape observables in heavy ion collisions // Journal of High Energy Physics. 2017. Vol. 2017. No. 7. P. 141.
14. **Park C., Jeon S., Gale C.** Jet modification with medium recoil in quark-gluon plasma // Nuclear Physics. A. 2019. Vol. 982. February. Pp. 643–646.
15. **He Y., Luo T., Wang X.N., et al.** Linear Boltzmann transport for jet propagation in the quark-gluon plasma: elastic processes and medium recoil // Physical Review. C. 2015. Vol. 91. No. 5. P. 054908.
16. **Chien Y.T., Vitev I.** Towards the understanding of jet shapes and cross sections in heavy ion collisions using soft-collinear effective theory // Journal of High Energy Physics. 2016. Vol. 2016. No. 5. P. 23.
17. **Chien Y.T., Emerman A., Kang Z.B., et al.** Jet quenching from QCD evolution // Physical Review. D. 2016. Vol. 93. No. 7. P. 074030.
18. **Ghiglieri J.** Energy loss at NLO in a high-temperature Quark-Gluon Plasma // Nuclear Physics. A. 2016. Vol. 956. December. Pp. 801–804.
19. **Djordjevic M., Zicic D., Blagojevic B., et al.** Dynamical energy loss formalism: from describing suppression patterns to implications for future experiments // Nuclear Physics. A. 2019.



Vol. 982. February. Pp. 699–702.

20. **Adcox K., Adler S.S., Aizama M., et al.** PHENIX detector overview // Nuclear Instruments and Methods in Physics Research. Section A: Accelerators, Spectrometers, Detectors and Associated Equipment. 2003. Vol. 499. No. 2–3. Pp. 469–479.

21. **Allen M., Bennett M.J., Bobrek M., et al.** PHENIX inner detectors // Nuclear Instruments and Methods in Physics Research. Section A: Accelerators, Spectrometers, Detectors and Associated Equipment. 2003. Vol. 499. No. 2–3. Pp. 549–559.

22. **Adler S.S., Allen M., Alley G., et al.** PHENIX on-line systems // Nuclear Instruments and Methods in Physics Research. Section A: Accelerators, Spectrometers, Detectors and Associated Equipment. 2003. Vol. 499. No. 2–3. Pp. 560–592.

23. **Miller M.L., Reygers K., Sanders S. J., et al.** Glauber modeling in high-energy nuclear collisions // Annual Review of Nuclear and Particle Science. 2007. Vol. 57. Pp. 205–243.

24. **Aphecetche L., Awes T.C., Banning J., et al.** PHENIX calorimeter // Nuclear Instruments

and Methods in Physics Research. Section A: Accelerators, Spectrometers, Detectors and Associated Equipment. 2003. Vol. 499. No. 2–3. Pp. 521–536.

25. **Tanabashi M., Hagiwara K., Hikasa K., et al.** Review of particle physics // Physical Review. D. 2018. Vol. 98. No. 3. P. 030001.

26. **Brun R., Hagelberg R., Hansroul M., et al.** Geant: simulation program for particle physics experiments. User guide and reference manual. Preprint CERN. CERN-DD-78-2-REV, 1978.

27. **Zharko S.** (PHENIX Collaboration). Studying parton energy loss using meson production in Large Collision Systems with PHENIX // Nuclear Physics. A. 2017. Vol. 967. November. Pp. 552–555.

28. **Aidala C., Ajitanand N.N., Akiba Y., et al.** Production of  $\pi^0$  and  $\eta$  mesons in Cu + Au collisions at  $\sqrt{s_{NN}} = 200$  GeV // Physical Review. C. 2018. Vol. 98. No. 5. P. 054903.

29. **Timilsina A.** (PHENIX Collaboration). PHENIX results on reconstructed jets in  $p + p$  and Cu + Au collisions // Nuclear Physics. A. 2016. Vol. 956. December. Pp. 637–640.

Статья поступила в редакцию 13.03.2019, принята к публикации 01.04.2019.

## СВЕДЕНИЯ ОБ АВТОРАХ

**БЕРДНИКОВ Александр Ярославич** – кандидат физико-математических наук, доцент кафедры экспериментальной ядерной физики Санкт-Петербургского политехнического университета Петра Великого.

195251, Российская Федерация, г. Санкт-Петербург, Политехническая ул., 29  
alexber@phmf.spbstu.ru

**БЕРДНИКОВ Ярослав Александрович** – доктор физико-математических наук, профессор, заведующий кафедрой экспериментальной ядерной физики Санкт-Петербургского политехнического университета Петра Великого.

195251, Российская Федерация, г. Санкт-Петербург, Политехническая ул., 29  
berdnikov@spbstu.ru

**ЖАРКО Сергей Вячеславович** – ассистент кафедры экспериментальной ядерной физики Санкт-Петербургского политехнического университета Петра Великого.

195251, Российская Федерация, г. Санкт-Петербург, Политехническая ул., 29  
zharkosergey94@gmail.com